2025, 65(11): 4860-4876
CSTR: 32112.14.j.AMS.20250235
DOI: 10.13343/j.cnki.wsxb.20250235

微生物学报
Acta Microbiologica Sinica
http://journals.im.ac.cn/actamicrocn

Research Article 研究报告

氮杂大环银/磺化壳聚糖络合物的抑菌性能和抗氧化活性

周依榆[1#]，练志峰[1#]，吕焱[1]，孙依薇[1]，吴惠香[1]，杨华[1,2]，黄建颖[1*]

1 浙江工商大学 食品与生物工程学院，浙江 杭州
2 广东海洋大学 食品科学与工程学院，广东 阳江

周依榆, 练志峰, 吕焱, 孙依薇, 吴惠香, 杨华, 黄建颖. 氮杂大环银/磺化壳聚糖络合物的抑菌性能和抗氧化活性[J]. 微生物学报, 2025, 65(11): 4860-4876.
ZHOU Yiyu, LIAN Zhifeng, LÜ Yan, SUN Yiwei, WU Huixiang, YANG Hua, HUANG Jianying. Antibacterial and antioxidant activities of Cage silver(I)/sulfonated chitosan complexes[J]. Acta Microbiologica Sinica, 2025, 65(11): 4860-4876.

摘　要：银纳米粒子的强抗菌活性主要归因于银离子的释放，银离子通过形成 Ag–S 键破坏细胞膜并导致关键酶失活。【目的】探索银离子的固定化策略以减少其释放。【方法】合成了一种含氮桥头的环状配体，并将其与银离子螯合，形成氮杂大环银配合物[Cage silver(I)]，随后将其与不同比例的磺化壳聚糖(sulfonate chitosan, SCS)进行络合，得到 SCS/Cage Ag(I)络合物(SCA**1**、SCA**2**、SCA**3**)，通过对金黄色葡萄球菌 (*Staphylococcus aureus*) ATCC 6538 和大肠杆菌(*Escherichia coli*) O157: H7 的最小抑菌浓度(minimum inhibitory concentration, MIC)和最小杀菌浓度(minimum bactericidal concentration, MBC)的测定、生物膜形成抑制等实验测定了它们的抗菌活性；同时通过还原能力、1,1-二苯基-2-苦肼基(1,1-diphenyl-2-picrylhydrazyl, DPPH)自由基和过氧化氢清除实验评估了它们的抗氧化性能。【结果】Cage silver(I)对 *S. aureus* ATCC 6538 的 MIC 为 0.015 mg/mL，MBC 为 0.031 mg/mL；对 *E. coli* O157:H7 的 MIC 为 0.031 mg/mL，MBC 为 0.120 mg/mL，显示出较强的抗菌活性。通过评估 DPPH 自由基抑制活性、过氧化氢清除活性以及还原能力发现 Cage silver(I)表现出显著的抗氧化性能，其对 DPPH 自由基的抑制率在 326 nm 和 517 nm 条件下分别为 42.2% 和 53.1%。Cage silver(I)显示出较高的抗菌和抗氧化活性，其次是 SCA**1**、SCA**2**、SCA**3** 和 SCS，这是由于 Cage silver(I)中银离子的含量比 SCA**1** 高 10 倍。此外，SCA**1** 的抗菌和抗氧化活性优于 SCS，进一步表明 SCS 中的磺酸基团可能与银离子发生强烈配位从而产生协同效应。【结论】通过结合银离子和 SCS 的优点可以在杀菌浓度下提高药物的生物利用度，减少其在环境中的积累，并最终降低治疗成本。本研究开发的方法为增强微生物控制能力并减少环境影响提供了一种可持续的策略。

资助项目：浙江省自然科学基金(LY20B040001)
This work was supported by the Zhejiang Provincial Natural Science Foundation (LY20B040001).
#These authors contributed equally to this work.
*Corresponding author. E-mail: huangjy@mail.zjgsu.edu.cn
Received: 2025-02-20; Accepted: 2025-04-10; Published online: 2025-06-05

关键词：Cage；银离子(I)；壳聚糖；抗生物膜形成；抗氧化活性

Antibacterial and antioxidant activities of Cage silver(I)/sulfonated chitosan complexes

ZHOU Yiyu[1#], LIAN Zhifeng[1#], LÜ Yan[1], SUN Yiwei[1], WU Huixiang[1], YANG Hua[1,2], HUANG Jianying[1*]

1 School of Food Science and Biotechnology, Zhejiang Gongshang University, Hangzhou, Zhejiang, China
2 School of Food Science and Engineering, Guangdong Ocean University, Yangjiang, Guangdong, China

Abstract: The potent antibacterial activity of silver nanoparticles is primarily attributed to the release of silver ions, which disrupt cell membranes and inactivate essential enzymes through Ag−S bonding formation. **[Objective]** To explore silver ion immobilization to minimize silver release. **[Methods]** A macrocyclic cryptand with nitrogen bridgeheads was prepared and subsequently chelated with silver ions to produce Cage silver(I), which was then coordinated with different ratios of sulfonated chitosan (SCS) to form SCS/Cage Ag(I) complexes (SCA**1**, SCA**2**, and SCA**3**). The antioxidant activities of the complexes were assessed by reducing power and 1, 1-diphenyl-2-picrylhydrazyl (DPPH) free radical and hydrogen peroxide scavenging assays. The antibacterial activities of the complexes were evaluated based on the minimum inhibitory concentrations (MICs) and minimum bactericidal concentrations (MBCs) against *Staphylococcus aureus* ATCC 6538 and *Escherichia coli* O157:H7 and the inhibition rate on biofilm formation. **[Results]** Cage silver(I) exhibited strong antibacterial activity, with the MIC of 0.015 mg/mL and MBC of 0.031 mg/mL against *S. aureus* ATCC 6538, and the MIC of 0.031 mg/mL and MBC of 0.120 mg/mL against *E. coli* O157:H7. Significant antioxidant properties of Cage silver(I) were also observed, as demonstrated by the DPPH free radical scavenging rates of 42.2% and 53.1% at 326 nm and 517 nm, respectively. Cage silver(I) exhibited the highest antibacterial and antioxidant activities, followed by SCA**1**, SCA**2**, SCA**3**, and SCS, because the content of silver ions in Cage silver(I) was 10-fold higher than that in SCA**1**. The antibacterial and antioxidant activities of SCA**1** were better than those of Cage silver(I), which further indicated that the sulfonic groups of SCS may intensely coordinate with silver ions to exert synergistic effects. **[Conclusion]** Combining the merits of silver ions and SCS improves the bioavailability of the agent at microbicidal concentrations, minimizes the accumulation in the environment, and reduces treatment costs. The method developed herein offers a sustainable approach to enhance microbial control while minimizing the impact on the environment.

Keywords: Cage; silver ion(I); chitosan; antibiofilm formation; antioxidant activity

The rapid appearance of antibiotic resistance, which creates a critical health menace worldwide, has generated renewed interest in developing products containing metals as an antibacterial agent[1-3]. As one of the valuable and common metals, silver and its complexes have been well used as potential agents in the medical field because of their antibacterial, anti-inflammatory, and anti-neoplastic properties. Most importantly, they exhibited good antibacterial activity, including antibiotic-resistant bacteria, fungi and parasites because of their multi-site action[1]. Metal ions are not only very rare for bacterial resistance but also possess a zombie effect[4-5]. Furthermore, these kinds of nanomaterials encapsulated by biodegradable polymer, such as chitosan, carboxymethyl cellulose, gelatin, and polylactic acid, can offer a potential approach for long-acting sterilization and controlled delivery[6]. Numerous functionalization of silver nanoparticles with a biocompatible biopolymer such as chitosan could improve their biological activities have been demonstrated[1].

The metal and metal-based ions have been extensively utilized in many anti-microbial applications for decades[7], possibly having an effect on different biochemical pathways of cells, involving in disrupting the function of normal cells, and generating irreversible damage. The high antibacterial activity of silver nanoparticles is supposed to release silver ions that destroy the cell membrane and inactive essential enzymes by Ag−S bonding[8]. Significant bactericidal activity of silver ion assisted with ebselen against multidrug-resistant uropathogenic *Escherichia coli* BC1 was demonstrated by consuming total intracellular glutathione (GSH), inhibiting thioredoxin reductase activity[9].

Subsequently, some ligands have been designed and prepared to bind with metal ions thereby regulating complex hydrophilicity or lipophilicity, stability, redox ability, as well as biological activity. Excellent antioxidant and antimicrobial activities of metals and metal-containing synthetic macrocyclic complexes allow them to have a wider range of biological applications[10]. For example, a series of N4-acrocyclic ligands with various substituted aromatic amines have been synthesized to chelate different metal ions[5,10]. Phenanthroline ligands complexed with transition metals [Mg(II), Cu(II), and Ag(I)] exhibited significant antibacterial activities[11].

The medicinal inorganic chemistry of silver coordination compounds is impressively versatile, and lots of published papers highlight the novel silver complexes as promising candidates for clinical trials and subsequent therapeutic use. Nevertheless, the little toxicity of those materials is indispensable. Their large-scale application has been limited because of their residual toxicity concerns. The typically silver-coordinated small molecule compounds might remain inside the body and then react with sulfur-containing proteins which exist in the bloodstream[4]. Therefore, it is imperative to develop an alternative approach for immobilizing silver ions into biomacromolecules to enhance antibacterial activity and mitigate cytotoxic effects. As a kind of anion biopolymer, sulfonate chitosan (SCS) with good water solubility, biocompatibility, biodegradability, antibacterial activity, and coordination potential makes its potential application in the biomedical fields[12]. Enhanced antibacterial properties, stability and low cytotoxicity were found after metal ions coordination with chitosan and its derivatives[5,13], such as AgBrNPs@copolymer-decorated CS[14],AgNPs@CS/SCS) [15], and cryptate copper(II)/SCS[5]. In this context, a new class of low-cost, easily synthesizable N4-acrocyclic ligand was prepared. After coordination with silver(I) followed by complexing with different ratios of SCS, their antioxidant and antimicrobial activities were investigated. The novelty of Cage silver(I)/SCS complexes developed herein may be fundamental in the selection of new metallo-drugs with very little or no toxicity to humans.

1 Materials and Methods

1.1 Materials and microorganisms

Chitosan (CS) with a deacetylation degree of 91% and a centipoise viscosity of 60 mPa·s (1.0%, 20 ℃) was afforded by Qingdao Honghai Biotechnology Company (Shandong, China). LIVE/DEAD® BacLight ™ Bacterial Viability Kit for microscopy was bought from ThermoFisher Scientific (Shanghai, China). Other chemical reagents and solvents were purchased from Aladdin Reagent Co., Ltd. (Shanghai, China) and were used directly without further purification.

1.2 Microorganism cultivation

The tested bacteria strains *Staphylococcus aureus* ATCC 6538 and *Escherichia coli* O157:H7 were bought from the China General Microbiological Culture (CGMCC, Beijing, China). Strains were respectively grown in Luria-Bertani (LB, Land Bridge, China) for *E. coli* and Trypticase-Soy-Broth (TSB, Land Bridge, China) supplemented with 1.0% glucose (Macklin, China) for *S. aureus*. All samples were incubated at 37 ℃ in a shaking incubator for 24 h, and the bacterial concentration was determined with a microplate reader (Tecan, Switzerland) at optical density (*OD*) of 600 nm (OD_{600}) of 1.0 corresponded to a concentration of 10^9 colony-forming units per-milliliter (CFU/mL)[16].

1.3 Apparatus and characterization

The ultraviolet-visible (UV-vis) spectra were measured with a spectrophotometer (Shimadzu, Japan) at room temperature (RT). Fourier transform infrared spectra (FT-IR) were recorded using a spectrometer (ThermoFisher Scientific, USA). High resolution electrospray ionization mass spectroscopy (HRMS) was determined on a TRAP instrument (A&B, USA). ^{1}H NMR spectra were recorded on a 500 MHz Bruker Avance NMR spectrometer (Bruker, Switzerland) at 25 °C. Silver ion concentrations were measured with a 2% nitric acid digestion method using an inductively coupled plasma mass spectrometer (ICP-MS, Agilent).

1.3.1 Synthesis of SCS[17] and Cage silver(I)

CS (1.0 g) was added to 80.0 mL of 2.0% aqueous acetic acid solution with stirring until completely dissolved. After 2.0 g of 1,3-propane sultone addition, the resulting mixture was further stirred for 6 h at 60 ℃ under a nitrogen atmosphere. After that, the solution was poured into cold acetone with vigorous stirring to precipitate white product. The white solid was washed with methylene chloride to remove unreacted 1,3-propane sultone and was vacuum-dried for 10 h.

The dinuclear silver complex was prepared according to the previous literature[18], which was illustrated in Figure 1. 0.48 g of benzene-1, 3-dicarboxaldehyde (3.60 mmol) was dissolved in 90.0 mL of acetonitrile (MeCN) solution. Then 0.37 g of tris(2-aminoethyl)amine (2.50 mmol) in 30.0 mL of MeCN was added dropwise with gently stirring for 10 h at RT. The resulting imine **1** was obtained (0.53 g, yield 75.5%) after filtration. Next, sodium borohydride (0.27 g, 7.00 mmol) was mixed with imines (0.18 g, 0.03 mmol), which were dissolved in 10.0 mL of methanol, and the mixture was stirred and refluxed overnight. The reaction completion was monitored by monitoring with thin-layer chromatography (TLC). After removal of the solvent, the residue was suspended in 12.0 mL of 2.00 mol/L ammonium chloride solution, then extracted with dichloromethane (12.0 mL) three times, and subsequently dried with Na_2SO_4. The resulting organic phases were evaporated under vacuum to afford Cage **2** (0.12 g, yield 69.2%).

Cage **2** (227.5 mg, 0.38 mmol) was dissolved in 40.0 mL of degassed MeCN/MeOH (4:1) followed by adding 132.5 mg of $AgNO_3$ (0.78 mmol). The mixture was stirred at RT for 10 h. After the removal of the solvent under reduced pressure, the residue was re-dissolved with 5.0 mL of MeCN. The resulting Cage silver(I) was precipitated by Et_2O addition (78.2 mg, yield 25.3%).

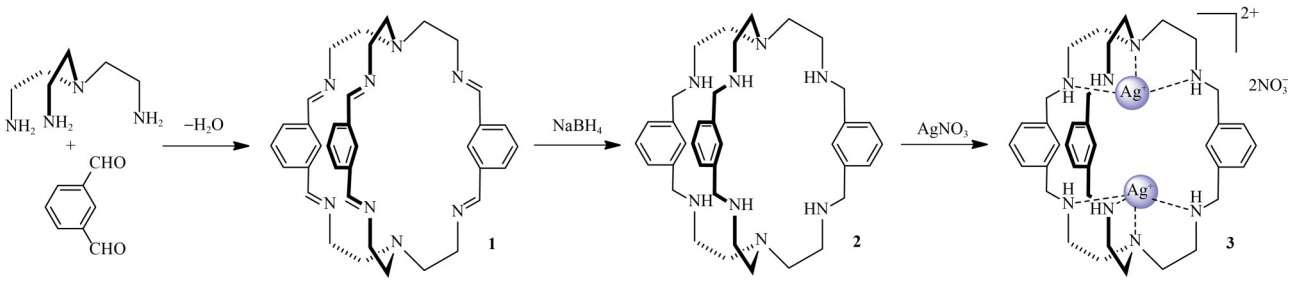

Figure 1 The synthesis procedures of Cage silver(I).

1.3.2 Preparation of SCS/Cage silver(I) (SCA) complex

Cage silver(I) was dissolved in DMSO at 1.0% (*W/V*) concentration in the final solution, while SCS was dissolved in Millipore water (Merck Millipore, Germany) with stirring at RT till complete dissolution. Then they were mixed with different weight ratios to afford SCS/Cage silver(I) 10:1 (SCA**1**), SCS/Cage silver(I) 20:1 (SCA**2**), and SCS/Cage silver(I) 30:1 (SCA**3**).

1.4 Minimal inhibitory concentration (MIC) and minimal bactericidal concentration (MBC) determination

MIC was determined by using the microtiter broth dilution method[12]. LB and TSB supplemented with 1.0% glucose were used as the negative controls, while strains with corresponding LB and TSB were served as the positive controls. An initial concentration of 4.0 mg/mL of SCA**1**, SCA**2**, and SCA**3** was serially diluted to 0.015 625, 0.031 25, 0.062 5, 0.125, 0.25, 0.5, 1.0, 2.0, and 4.0 mg/mL, and SCS was from 0.039 062 5 to 10.0 mg/mL, while the concentrations of Cage Ag ranged from 0.007 812 5 to 0.5 mg/mL. 100 μL of each solution was added to 96-well plates, followed by the addition of 100 μL of bacterial suspension (10^6 CFU/mL). All inoculated microplates were incubated at 37 ℃ for 24 h, followed by the absorbance values read at OD_{600} with a microplate reader (Tecan, Switzerland). The MIC was determined as the lowest concentration that showed complete inhibition of visible growth.

Tryptic-Soy-Agar (TSA, Land Bridge, China) plates were applied for MBC value determination according to the number of colony-forming units[12]. All samples were performed in triplicate.

1.5 Biofilm formation inhibition

1.5.1 Adhesion assay

The effects of all samples on the biofilm formation were determined according to the previous literature[12]. Briefly, the activated *E. coli* and *S. aureus* suspensions (10^8 CFU/mL) were separately pre-mixed with 10.0 mL of the test compound solutions to achieve final compound concentrations ranging from 1MIC concentration to 1/4MIC concentration. The sterilized 1 cm^2×1 cm^2 cover glass was pre-placed in well plates, then an aliquot of 2.0 mL of the cell/compound mixtures was added for replicate testing. After 48 h of biofilm formation in the 24-well plates, the cover glass was gently removed from the plates and subsequently rinsed with sterile phosphate buffer saline (PBS, 0.01 mol/L, pH 7.4) to remove non-adherent cells. Then, the rinsed cover glass was placed in a centrifuge tube containing 2.0 mL normal saline, and ultrasound was performed for 5 min at 150 W power. Followed by shaking with a vortex oscillator for 1 min, 100.0 μL of the oscillating bacterial solution was added to TSA plates for general colony count.

1.5.2 Confocal laser scanning microscopy (CLSM)[5]

The *E. coli* and *S. aureus* cells treated with or without different samples were grown in a confocal FluroDish petri dish with TSB (1.0% glucose, 3.0 mL), and then 1.0% suspension (10^7 CFU/mL) of stains was separately added to the final concentrations of the samples were 1MIC.

Sterilized deionized water without samples was used as a control. After 48 hours incubation at 37 ℃, the planktonic bacteria on the surface of the plate was gently rinsed with sterile PBS (pH 7.4). Then, all bacterial cells were stained with SYTO9 and propidium iodide (PI), the viability of corresponding cells was assessed by using a LIVE/DEAD® Bacterial Staining Kit (ThermoFisher Scientific), and the distribution of live and dead bacteria in biofilms were observed by a CLSM (Zeiss, Germany).

1.6 DPPH radical scavenging activity

A stable free radical DPPH was used to evaluate the scavenging effect of all resulting complexes according to the previous reports[19-20]. 1.0 mL of each different concentrations sample solution was separately mixed with 9.0 mL of ethanol solution of DPPH (200.0 μmol/L) to afford a solution of DPPH with a final concentration of 100.0 μmol/L. The mixture was reacted in a water bath at 25 °C for 30 min, then the absorbance of the resulting reaction was read from 200 nm to 800 nm by a spectrophotometer (Shimadzu, Japan). The DPPH radical scavenging activity was expressed as a percentage of inhibition activity according to Equation (1).

$$\text{Inhibition} = (A_0 - A_X)/A_0 \times 100\% \quad (1)$$

where A_0 is the absorbance of the control and A_X is the absorbance of different concentrations samples. All samples were measured in triplicate.

1.7 Reducing power assay[19]

1.0 mL of each different concentrations sample solutions ranging from 0 mg/mL to 4.0 mg/mL were respectively mixed with 0.2 mL of fresh PBS (0.2 mol/L, pH 6.6) and 1.0 mL of 1.0% potassium ferricyanide. The mixtures were stirred at 50 ℃ for 20 min, respectively. After 1.0 mL of 10% trichloroacetic acid addition, the resulting reaction mixtures were centrifuged at 6 000 r/min for 10 min (Cence). 2.0 mL of each supernatant was collected and added with 0.35 mL of 3.0% ferric chloride solution and 1.0 mL of distilled water, followed by the absorbance that read at 700 nm. Reducing power can be evaluated by the increased absorbance of the reaction mixture. All samples were assayed in triplicate.

1.8 Scavenging of hydrogen peroxide[21]

The sample solution (4.0 mg/mL) was mixed with 2.4 mL of 0.1 mol/L PBS (pH 7.4), followed by adding 0.6 mL of 43.0 mmol/L solution of hydrogen peroxide. The absorbance was measured at 230 nm from 0 min to 40 min and at every 5 min interval until 240 min. While a separate blank without hydrogen peroxide solution was served as background subtraction. The radical scavenging ability was expressed as a percentage of scavenging activity against hydrogen peroxide according to Equation (2).

$$\text{Inhibition} = 1 - (A_0 - A_X)/(A_0' - A_X') \times 100\% \quad (2)$$

where A_0 and A_0' are the absorbance read at the initial incubation time for the sample and control, respectively, and A_X and A_X' are the absorbance of sample and control read at successive time, respectively. All samples were assayed in triplicate.

1.9 Statistical analysis

Analysis of variance (ANOVA) (P<0.05) was performed using SPSS 27 software. The display data was expressed as the means±SD. All experiments were performed at least three times. Differences at P<0.05 were considered to be statistically significant.

2 Results

2.1 Characterization

As illustrated in Figure 1, Cage silver(I) was prepared using benzene-1, 3-dicarboxaldehyde and tris(2-aminoethyl)amine as starting materials, followed by a reduction reaction using sodium borohydride as a reducing agent, and subsequently coordinated with silver ions. Its structure was characterized by ^{1}H NMR and HRMS (high-resolution mass spectroscopy) spectra. The ^{1}H NMR spectra of Cage and Cage silver(I) were presented in Figure 2, which confirmed their formation.

The structure of the Cage silver(I) complex was further supported by HRMS. The ESI-MS of

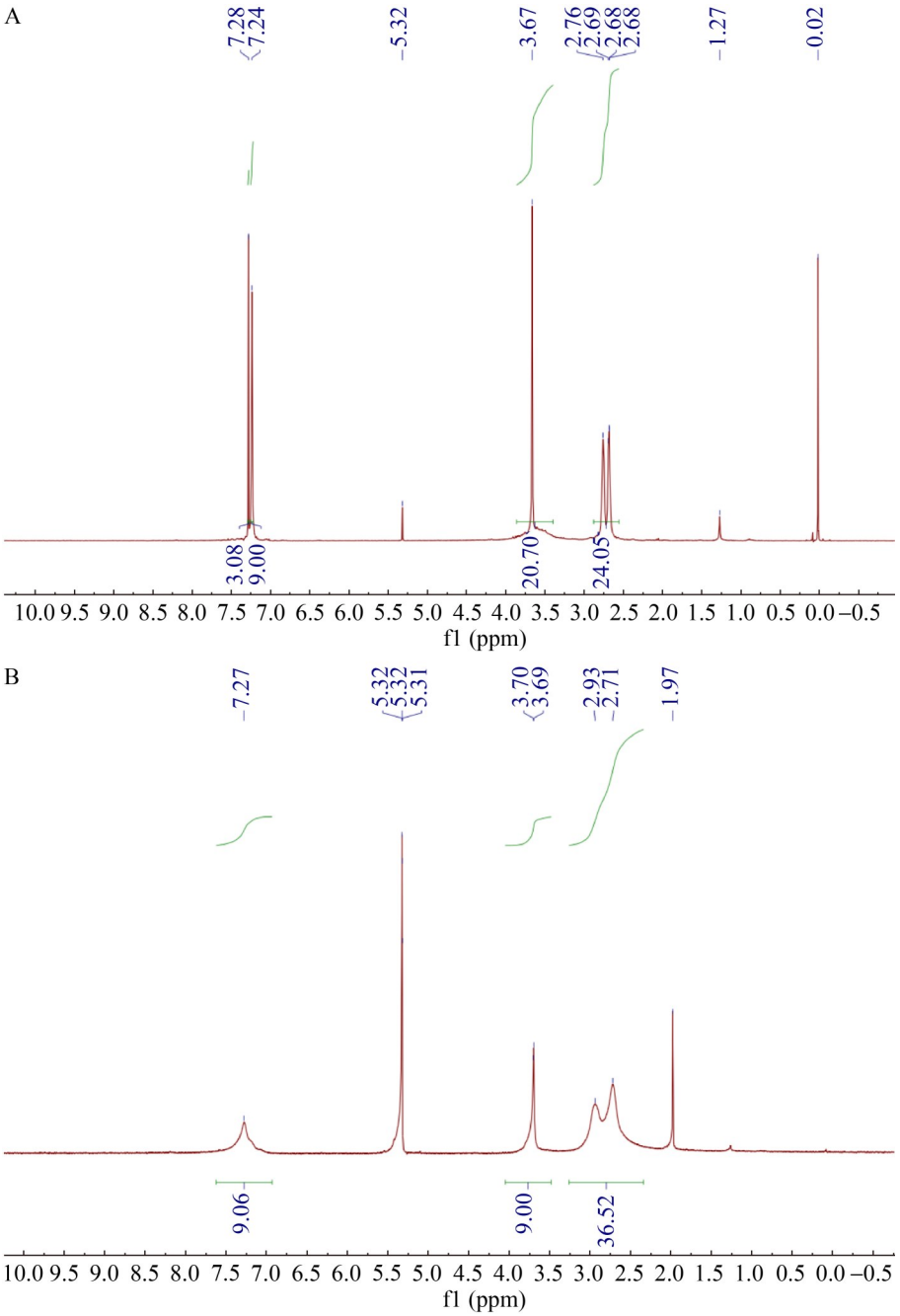

Figure 2 ^{1}H NMR spectra of Cage (A) and Cage silver(I) (B). Cage: ^{1}H NMR (500 MHz, $CDCl_3$) δ 7.28 (s, 3 H), 7.24 (s, 9 H), 3.67 (s, 20 H), 2.68 (m, 24 H); Cage silver(I): ^{1}H NMR (500 MHz, CD_2Cl_2) δ 7.27 (s, 9 H), 3.70 (m, 9 H), 2.85 (m, 36 H).

Cage silver(I) (Figure 3) showed related peaks at *m*/*z*=407.130 4 and *m*/*z*=705.354 1, corresponding to $[M_{cage}+2Ag]^{2+}$ and $[M_{cage}+Ag]^{+}$, respectively. These two peaks were isotopically resolved and agreed very well with their calculated isotopic distributions.

The silver ion concentrations of each sample analyzed by ICP-MS were 247.74, 20.49, 8.71, and 7.84 μg/mL corresponding to Cage silver(I), SCA**1**, SCA**2**, and SCA**3** (Table 1).

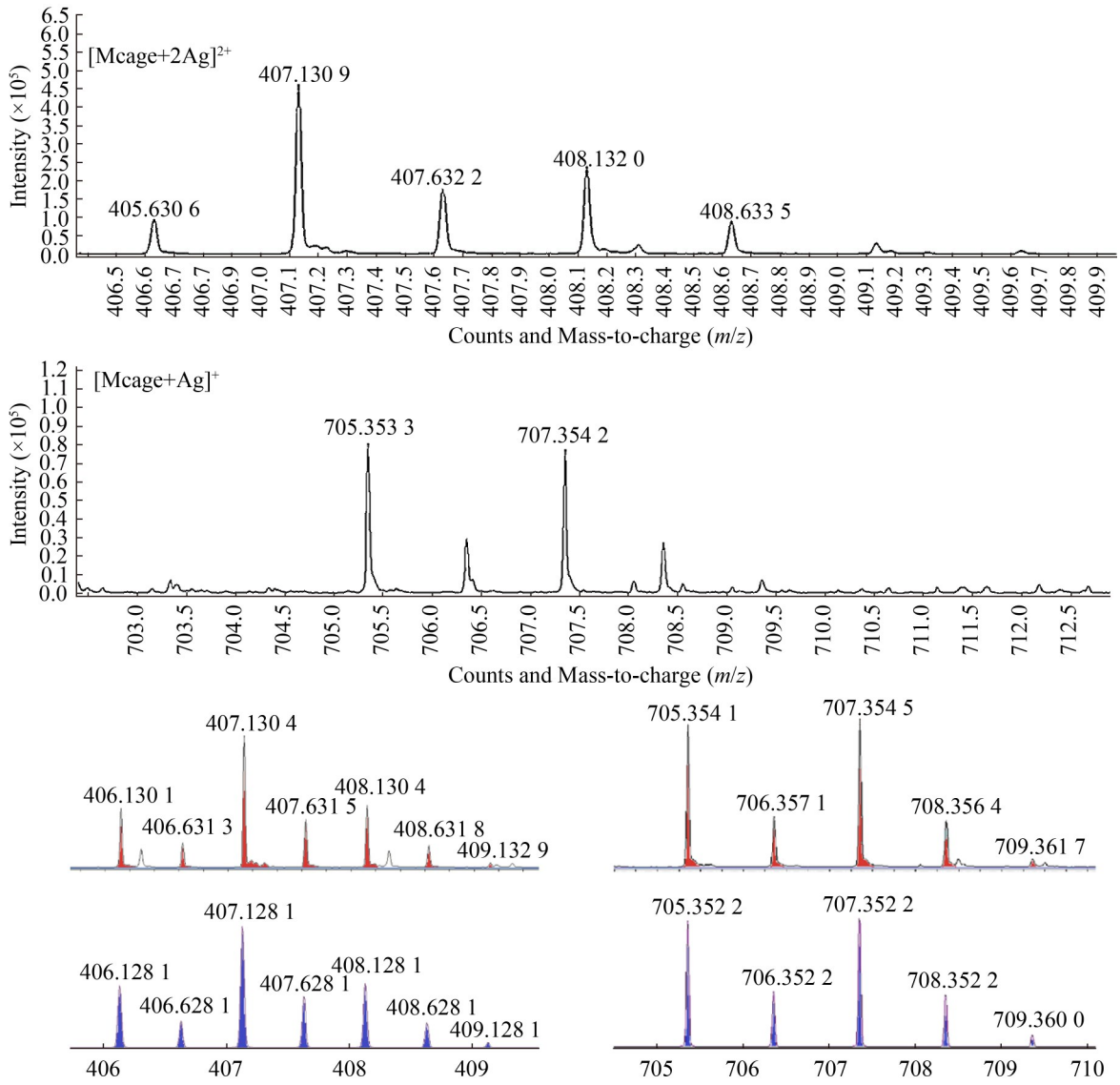

Figure 3 HRMS of the Cage silver(I) (top, red) and their simulated spectra (bottom, blue). $[M_{cage}+2Ag]^{2+}$: HRMS (ESI/Q-TOF) *m/z*: $[M_{cage}+2Ag]^{2+}$ Calcd for $C_{36}H_{54}Ag_2N_8^{2+}$ 407.128 1, Found: 407.130 4; $[M_{cage}+Ag]^{+}$: HRMS (ESI/Q-TOF) *m/z*: $[M_{cage}+Ag]^{+}$ Calcd for $C_{36}H_{54}AgN_8^{+}$ 705.352 2, Found: 705.354 1.

Table 1 The designed composition ratio and silver ion content of samples

Samples	Cage silver(I) (1.0 mg/mL) (mL)	SCS (1.0 mg/mL) (mL)	Silver ion content (μg/mL)
Cage silver(I)	1.0	0.0	247.74
SCA1:10	1.0	10.0	20.49
SCA1:20	1.0	20.0	8.71
SCA1:30	1.0	30.0	7.84

To further illustrate the structure and interaction between functional groups of Cage silver(I), SCS, and formation of SCA, all ground and dried samples were examined in the infrared range (4 000 cm^{-1} to 400 cm^{-1}) by a FT-IR spectrophotometer, and the results were shown in Figure 4. FT-IR spectrum of SCS showed the typical stretching vibration peaks of secondary N−H and O−H of SCS appeared around 3 440 cm^{-1}, N−H stretching vibration at 1 646 cm^{-1} was attributed to the acetylated units of chitosan, S=O stretching vibration and O=S=O symmetric vibration of sulfonic acid group were at 1 180 cm^{-1} and 1 030 cm^{-1} (Figure 4A) which was following the previous report[11].

As to Cage (Figure 4C), the bands appeared at 2 945 cm^{-1} and 2 821 cm^{-1} accounted for C − H stretching vibration of methylene, and at 1 451 cm^{-1} was C − H bending vibration band of methylene. The present of the band at 3 030 cm^{-1} was supposed to the C − H stretching vibration of the benzene ring. While the bands at 803 cm^{-1} and 711 cm^{-1} are attributed to the bending vibration of C−H in the benzene ring. The band at 1 615 cm^{-1} corresponded to the C=C stretching vibration of the benzene ring. After chelator with silver ions, the N − H vibrational bands of Cage at 3 431 cm^{-1} shifted to 3 449 cm^{-1}, The sharp peak appeared at 3 266 cm^{-1} possibly ascribed to the stretching vibration of C=C − H of benzene, while sharp peak around 2 839 cm^{-1} was C−H vibration of Cage silver(I). When Cage silver(I) complexed with SCS, the typical secondary N − H stretching vibration peak at 3 426 cm^{-1}, C=C−H of benzene at 3 226 cm^{-1}, and N − H bend near 1 647 cm^{-1} ascribed to amine groups and acetylated units of chitosan could be seen from the FT-IR spectrum of SCA**1** (Figure 4B). The decrease in peak intensity of Cage silver(I) at 1 358 cm^{-1} was evidence of the Cage silver(I) complexed with SCS.

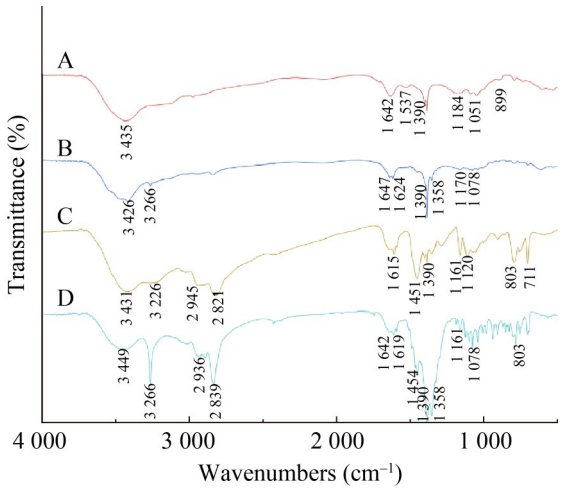

Figure 4 FT-IR spectra of SCS (A), SCA**1** (B), Cage (C), and Cage silver(I) (D).

2.2 Antibacterial activity

The antibacterial activities of all samples against *S. aureus*, and *E. coli* were investigated by MIC and MBC determination, while methicillin against *S. aureus* and polymyxin B against *E. coli* were used as controls. As presented in Table 2 and Figure 5, the growth of *S. aureus* and *E. coli* was inhibited by Cage silver(I) at 0.015 mg/mL and 0.031 mg/mL, with the corresponding MBC values 0.031 mg/mL and 0.120 mg/mL, respectively. Apparently, the antibacterial activities of all tested samples gradually reduced when the content of Cage silver(I) decreased in SCA complexes, indicating it played an important role in the bacteriostatic capability of SCA. The MIC and MBC of SCA**1** were 0.12 mg/mL and 0.50 mg/mL against *S. aureus*, 0.12 mg/mL and 0.25 mg/mL against *E. coli*, exhibiting stronger antibacterial activities than those of SCS with 0.62 mg/mL and 5.00 mg/mL against *S. aureus*, 0.62 mg/mL and 2.50 mg/mL against *E. coli*, which was consistent

Table 2 The MIC and MBC of different samples against *Escherichia coli* and *Staphylococcus aureus*

Sample	*E. coli* (mg/mL)		*S. aureus* (mg/mL)	
	MIC	MBC	MIC	MBC
Cage silver(I)	0.031	0.12	0.015	0.031
SCS	0.620	2.50	0.620	5.00
SCA**1**	0.120	0.25	0.120	0.50
SCA**2**	0.120	0.50	0.250	1.00
SCA**3**	0.250	1.00	0.500	2.00

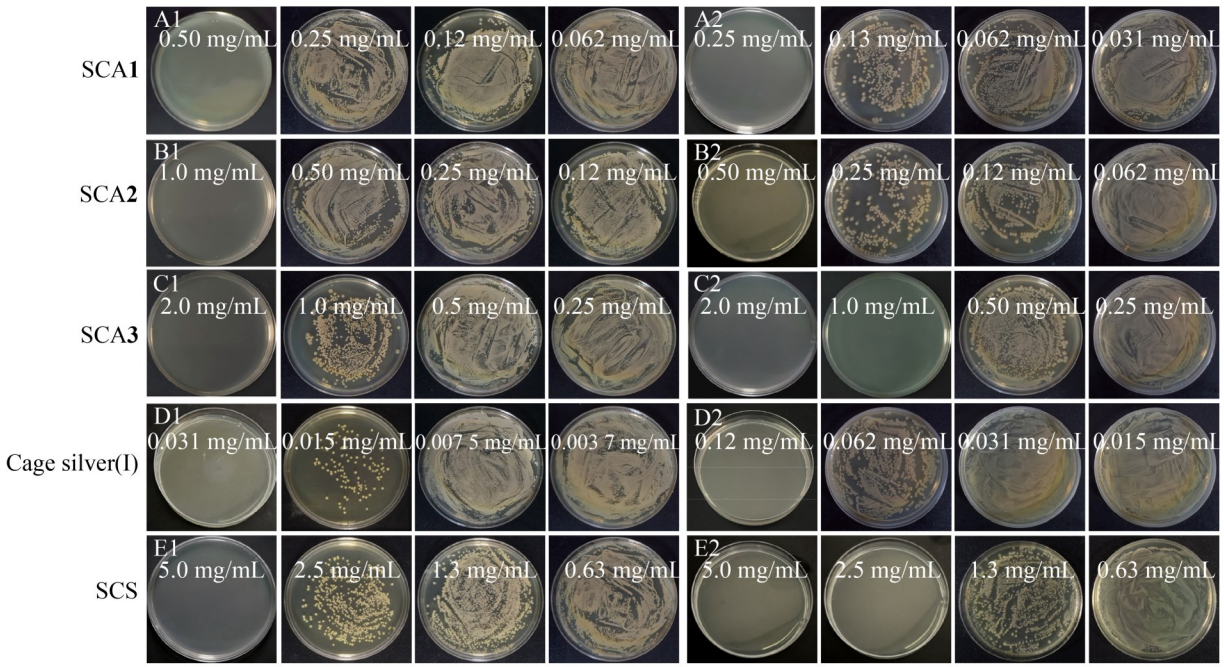

Figure 5 Bactericidal effect of SCA**1** (A1, A2), SCA**2** (B1, B2), SCA**3** (C1, C2), Cage silver(I) (D1, D2) and SCS (E1, E2) on *Staphylococcus aureus* (left) and *Escherichia coli* (right).

with a previous study[22].

2.3 Antiadhesion and antibiofilm formation

All samples exhibited adhesion inhibitory properties against *E. coli* and *S. aureus* with Cage silver(I) content-dependent mode (Figure 6). As expected, Cage silver(I) showed the best anti-adhesion among all tested samples. The colony forming units of *E. coli* and *S. aureus* were 3.90 lg CFU/cm^2 and 4.16 lg CFU/cm^2 when 1MIC Cage silver(I) treated, followed by SCA**1** (4.60 lg CFU/cm^2 and 4.45 lg CFU/cm^2), SCA**2** (4.98 lg CFU/cm^2 and 5.14 lg CFU/cm^2), SCA**3** (4.89 lg CFU/cm^2 and 5.75 lg CFU/cm^2), SCS (5.34 lg CFU/cm^2 and 5.70 lg CFU/cm^2), and the control (8.44 lg CFU/cm^2 and 8.69 lg CFU/cm^2). It is found that *S. aureus* was more susceptible to Cage silver(I) than *E. coli*, while SCA**1**, SCA**2**, SCA**3**, and SCS exhibited better anti-adhesion activities against *E. coli* than against *S. aureus*.

2.4 CLSM

As shown in Figure 7A, the distribution of *S. aureus* biofilm in the control group was dense and uniform with good cell activity. Less green fluorescence intensity and more reddish fluorescent cells (Figure 7B) were found compared with the control in the confocal microscopy imaging of *S. aureus* treated with SCS. Importantly, rare fluorescence intensity was observed in Cage silver (I) treated *S. aureus* (Figure 7D), followed by SCA**1** treatment (Figure 7C). Similar effects of the tested samples against *E. coli* biofilm can be seen from Figure 8A−8D, indicating that Cage silver(I) exhibited the strongest anti-biofilm formation activity against *E. coli* and *S. aureus* among SCA**1** and SCS at MIC concentration.

Dramatic reduction of the cell viability and density illustrated that Cage silver(I) could inhibit the adhesion of *S. aureus* and *E. coli* to the coverslip surfaces, which was followed by SCA**1** and SCS. These results were consistent with the results of the bacterial biofilm adhesion (Figure 6).

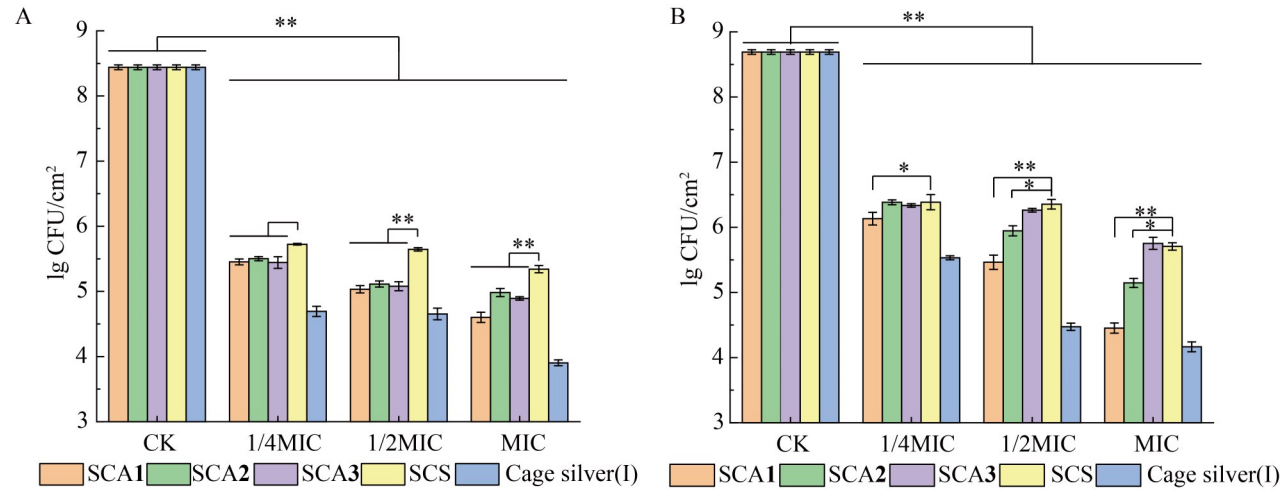

Figure 6 Effects of SCA1, SCA2, SCA3, SCS, and Cage silver(I) on the adhesion of *Escherichia coli* (A) and *Staphylococcus aureus* (B). *: $P<0.05$; **: $P<0.01$.

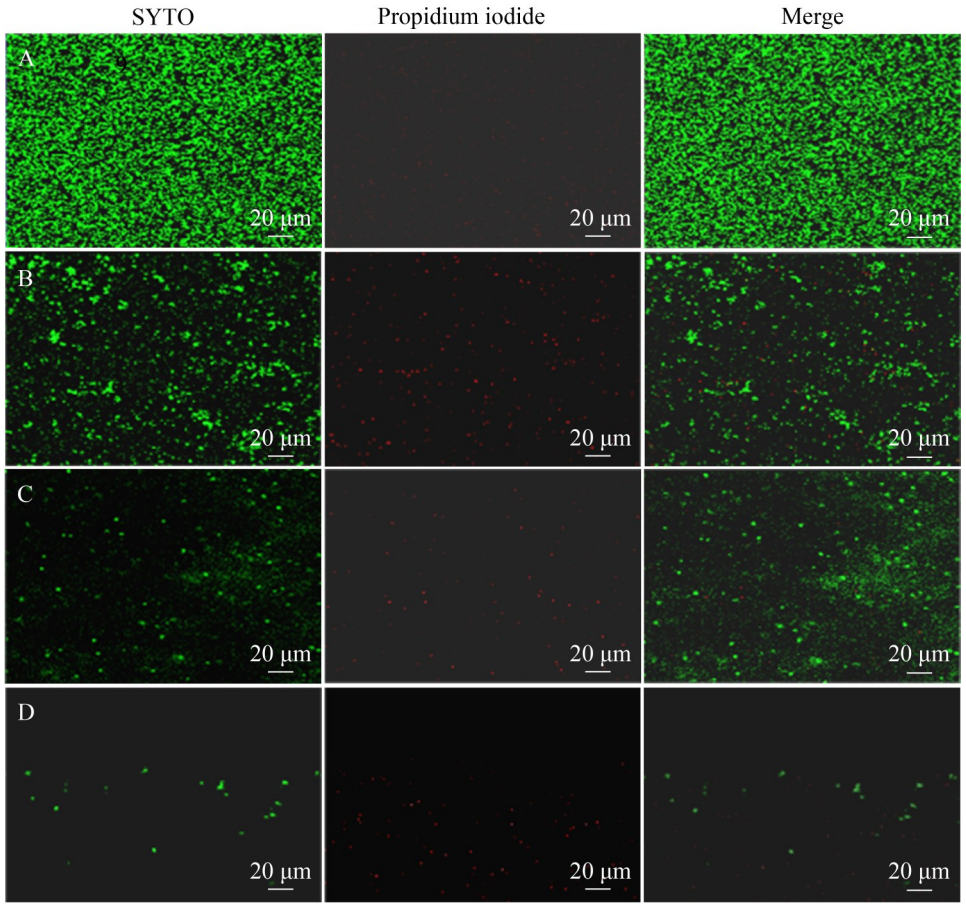

Figure 7 CLSM images of *Staphylococcus aureus* with TSB+1.0% glucose. A: control; B: SCS (0.62 mg/mL) treated; C: SCA**1** (0.12 mg/mL) treated; D: Cage silver(I) (0.015 mg/mL) treated.

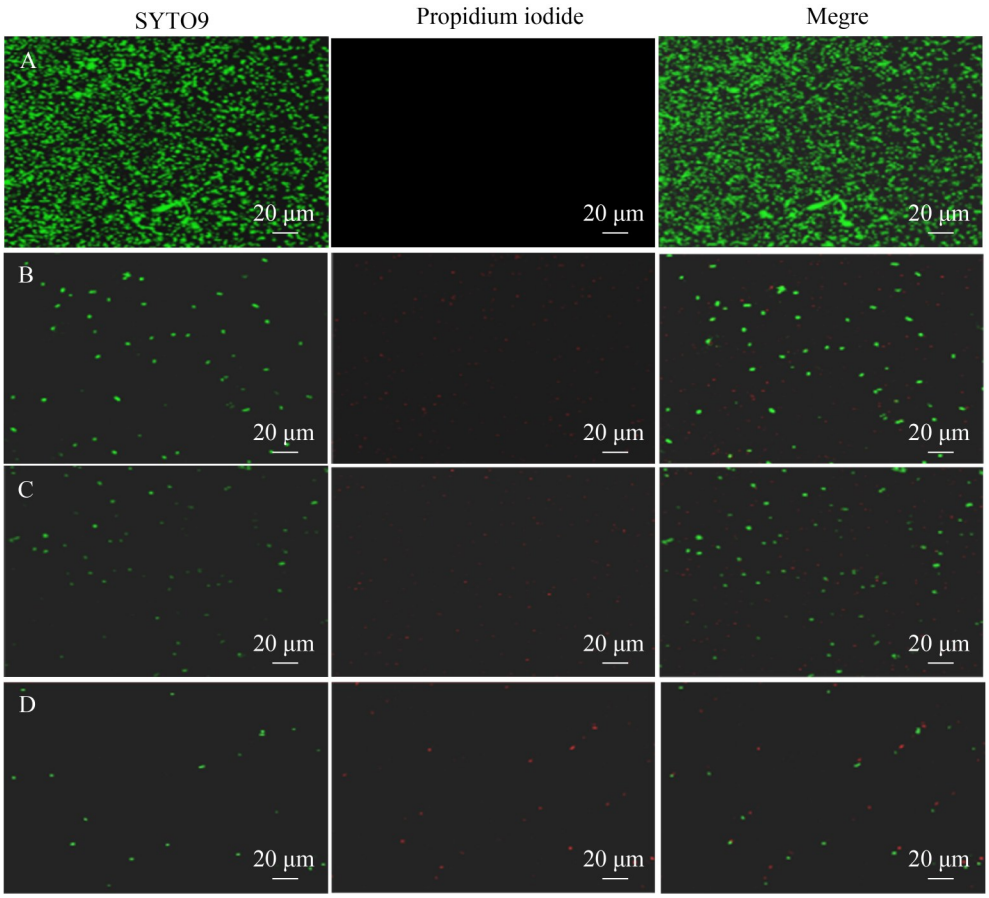

Figure 8 CLSM images of *Escherichia coli* with LB+1.0% glucose. A: control; B: SCS (0.62 mg/mL) treated; C: SCA**1** (0.12 mg/mL) treated; D: Cage silver(I) (0.031 mg/mL) treated.

2.5 DPPH radical scavenging determination

DPPH, a semi-stable free radical, is a radical scavenger because it is capable of accepting electrons from reactive radicals. The mechanism of DPPH free radical scavenging may be very complex because the DPPH molecules cannot only react with electrophile reagents but hydroxyl radicals, indicating that the absorbance of DPPH absorption bands at 517 nm and 326 nm, possibly change simultaneously (Figure 9A). Therefore, the determination of radical scavenging ability of compounds was recorded based on photobleaching of DPPH at 517 nm and 326 nm is reasonable[19].

Figure 9 showed a set of UV-vis spectra measured upon DPPH solution reacting with various samples. It can be clearly seen that different absorbance decreases of DPPH absorption bands at 517 nm and 326 nm occurred with a concentration-dependent mode in the DPPH radical scavenging activity assessment of all tested samples (Figure 9 and Table 3).

A substantial and statistically significant decrease in the DPPH levels of all samples can be seen from Table 3. Cage silver(I) exhibited the strongest antioxidant activity among all tested samples, and its inhibition percentages of DPPH radicals reached 42.2% and 53.1%, respectively, based on the photobleaching of DPPH at 326 nm and 517 nm. The inhibitory activities of SCA**1**, SCA**2**, and SCA**3** were 43.9%, 35.0%, 16.3% at 326 nm, and 46.4%, 36.2%, 20.3% at 517 nm at the

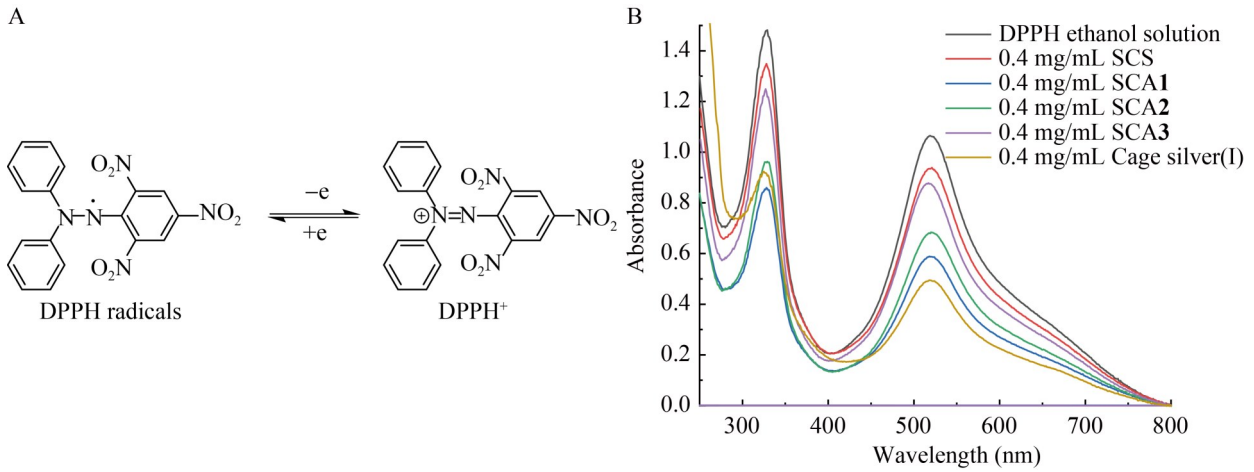

Figure 9 DPPH determination. A: Chemical structures of DPPH radical and its conjugated oxidation product; B: UV-vis spectra of the different tested samples at 0.4 mg/mL and DPPH ethanol solution.

Table 3 Inhibition percentages of DPPH radicals by the samples

Wave length (nm)	Inhibition percentages (%)				
	Sample	0.1 mg/mL	0.2 mg/mL	0.3 mg/mL	0.4 mg/mL
326	SCS	8.97±2.03a	9.71±1.21a	9.98±1.12a	10.99±1.13a
	SCA**1**	40.55±1.22c	41.90±3.12d	42.78±2.12d	43.85±3.12d
	SCA**2**	17.81±3.34a	27.12±1.45c	28.87±2.12c	35.02±3.31c
	SCA**3**	12.48±3.23a	13.22±1.12b	14.71±1.16b	16.26±2.12b
	Cage silver(I)	37.31±1.08b	38.39±1.11d	41.36±3.14d	42.24±4.24d
517	SCS	11.54±3.26a	12.30±4.46a	13.14±2.22a	14.46±3.21a
	SCA**1**	42.62±2.62b	43.19±3.22c	45.35±2.69d	46.47±3.26d
	SCA**2**	17.84±4.15a	29.48±1.12b	30.32±2.23c	36.24±3.51c
	SCA**3**	13.80±2.21a	15.11±1.21a	17.18±1.12b	20.37±1.12b
	Cage silver(I)	42.34±3.92b	44.88±2.22c	52.01±3.61e	53.14±2.31e

Different lowercase letters in each group indicate a significant difference at $P<0.05$ in the same concentration of different treatments (Duncan's test).

concentration of 0.4 mg/mL. While the inhibitory activity of SCS against DPPH was 11.0% and 14.5% based on photobleaching of DPPH at 326 nm and at 517 nm when the concentration of SCS was 0.4 mg/mL.

2.6 Reducing power

As shown in Figure 9, the reducing power of all samples was in concentration-dependent manner. Significant reducing power of Cage silver (I) could be observed from Figure 9. When the concentration was 0.4 mg/mL, the reducing power of Cage silver(I) was up to 1.85. As expected, the reducing power was reduced in order of SCA**1**, SCA**2**, and SCA**3**, which were 0.58, 0.29 and 0.27 when the concentration of samples was 0.4 mg/mL, while the reducing power of SCS was 0.09 at 0.4 mg/mL. The antioxidant capacity of SCS was due to their hydrogen-donating ability[23]. However, the maximum absorbance was observed for Cage silver(I) which was supposed to the presence of nitrogen and silver atoms in Cage silver(I).

2.7 Scavenging activity of hydrogen peroxide

As shown in Figure 10, the scavenging activity of samples was directly correlated with the reaction time, which reached 57.3%, 49.8%, 38.9%, and 37.4% of SCA**1**, SCA**2**, SCA**3**, and SCS, respectively, in 40 min reaction. The scavenging ability of Cage silver(I) against hydrogen peroxide was not shown herein because high concentrations of silver ions in Cage silver(I) reacted with hydrogen peroxide to produce silver oxide[19].

3 Discussion

Silver is less toxic to human cells, however, a growing environmental concern in the increasing silver level accumulation after long intensity of exposure will produce residual toxicity and ultimately be harmful to public health. Herein, N4-acrocyclic ligand (Cage**2**) was successfully synthesized, and was confirmed by ^{1}H NMR spectra which were following the literature[18]. Then the silver ions were tightly chelated in the nitrogen macrocyclic and further mixed with the SCS, addressing new materials which can alleviate silver release.

After structure characterization by ^{1}H NMR, HRMS, and FT-IR, the antibacterial and antioxidant activities of prepared Cage silver(I), and SCA were studied. As expected, Cage silver(I) exhibited excellent antibacterial activities against *S. aureus* and *E. coli* with the lowest MIC and MBC values (0.015 mg/mL and 0.031 mg/mL), followed by SCA**1**, SCA**2**, SCA**3**, and SCS, indicating that the content of Cage silver(I) played an important role in bacteriostatic capability of SCA. Similar trend of antibiofilm formation ability present in CLSM further demonstrated the significantly important Cage silver(I) content in SCA. These results are in accordance with the previous report[5]. While the MIC values of methicillin against *S. aureus* and polymyxin B against *E. coli* with 0.76 mg/L and 2.60 mg/L[16], respectively, show slightly better than Cage silver(I), however, both are easy to develop resistance, and the resistance development of SCA is worthy to be assessed.

Additionally, commercially available silver-based disinfectants such as silver nitrate[24] and nano-silver particles[25] exhibited antibacterial activities with the MIC values ranging from 0.01 mg/mL to 0.04 mg/mL for silver nitrate against *S. aureus* and *E. coli*, and 12.5 mg/mL to 25.0 mg/mL for nano-silver particles against *S. aureus* and *E. coli*, further demonstrated that silver ions played a key bactericidal role, which was

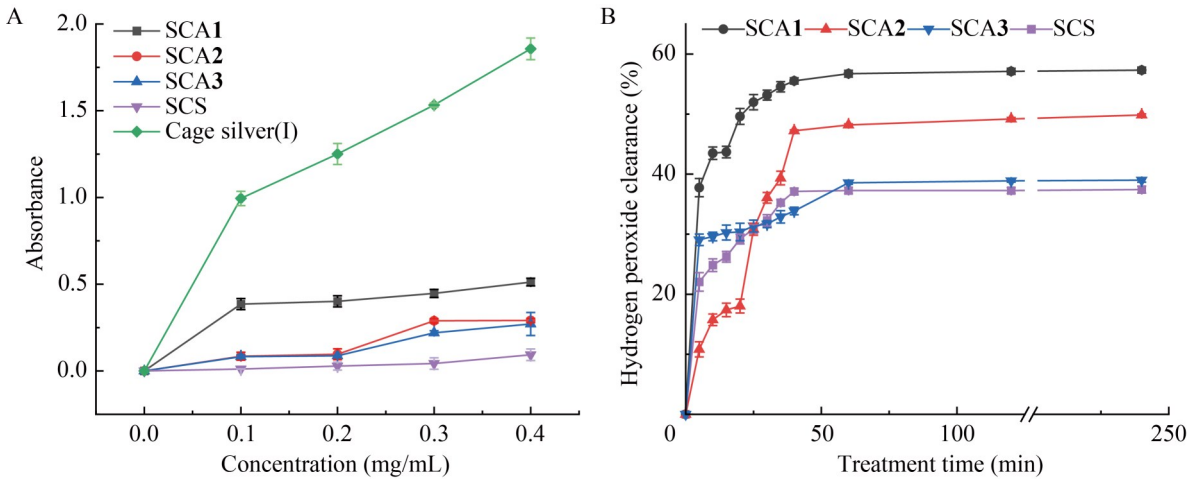

Figure 10 Antioxidant activity assays. Reducing power (A) and hydrogen peroxide scavenging activity (B) of SCA**1**, SCA**2**, SCA**3**, SCS and Cage silver(I).

following the previous study[26]. Herein, the MICs of Cage silver(I) and SCA**1** against *S. aureus* and *E. coli* were 0.015 mg/mL and 0.12 mg/mL, indicative of their significant inhibitory activities. The mode of antimicrobial action of silver ions is supposed to bind to the surface of the bacterial cell membrane and subsequently enter into cell to interfere with the activity of essential intracellular enzymes and DNA, causing enzyme degradation, cell protein inactivation, and DNA breakage, eventually resulted in the bacteria's death[2,27]. Evidence also suggests that the antimicrobial activity of silver ions may be related to the redox reaction which impairs the cell cytoplasm, leading to inhibition of cell replication and cell death[7,27]. Therefore, the efficiency of the antibacterial activity of silver complex depends upon the content of silver ions, which were exposed to the bacteria[7]. Both chemisorbed Ag^+ and AgNP aggregation would influence their antibacterial efficacy[28], however, AgNP and silver ions can easily migrate to the environment, ultimately threatening human health.

In our study, the silver ions bound to the four nitrogen atoms at the trend end of the macro-bicyclic cryptand, making the coordination geometry very distorted, in which all four nitrogen atoms were on one side of the metal ion which has been reported by Ray and Bharadwaj[29]. Importantly, the spherically symmetric configuration of the silver(I) ion allows the coordination number to the Cage is 2 which was proved by ESI-MS. All these factors influenced both the electronic and steric properties of Cage silver(I), which in turn modulated the rate of silver release, also maintaining their bioavailability over an extended period and preventing reinfection or resistance. The proposed antibacterial mechanism of SCA is that silver and SCS can bind bacterial cell membrane, destroy the cell wall, and induce oxidative damage of lipid and protein present in cells.

Additionally, overproduction of activated oxygen species is one of the major contributors to oxidative damage of DNA, lipids and proteins, which increases the chance of cancer, aging, inflammation, as well as cardiovascular diseases. Many transition metal complexes also showed significant antioxidant activities[30]. The N4-acrocyclic ligand synthesized in our study had the ability to chelate with silver ions, subsequently complex with SCS. Herein, significant antioxidant activities of Cage silver(I) and SCA were demonstrated by the reducing power, DPPH radical, and hydrogen peroxide scavenging assays (Table 3, Figure 9, and Figure 10).

Based on the antibacterial and antioxidant activities assessment, Cage silver(I) exhibited the highest antibacterial and antioxidant activity followed by SCA**1**, SCA**2**, SCA**3**, and SCS, which was because the content of silver ions in Cage silver (I) was 10-fold higher than that of SCA**1** (Table 1). While the antibacterial and antioxidant activity of SCA**1** was less than 10-fold those of Cage silver(I), further indicating that the amino sulfonic groups of SCS may be intensely coordinated with silver ions, which would be helpful for synergistic effects. The potent antibacterial and antioxidant activities of SCA were in agreement with the results of polysaccharide-based silver nanoparticles and plant extract-based silver nanoparticles[31-33].

4 Conclusion

In this study, Cage silver(I) was prepared and complexed with SCS. After characterization by NMR, FT-IR, HRMS, and ICP-MS analysis, the antibacterial activity and antioxidant capacity assay of all samples were investigated. The mass ratio of 10:1 between SCS and Cage silver(I) was considered as the optimal ratio by determining the antibacterial activities against *S. aureus* and *E. coli*. Also, the study discovered that the complex of SCS and Cage silver(I) exhibited a remarkable ability to counteract free radicals as an antioxidant, according to the scavenging capacities against DPPH, reducing power and scavenging of hydrogen peroxide. The chitosan matrix not only exerted synergistic effects but also mitigated the

toxicity produced by silver ion release and ultimately reduced environmental accumulation. Notably, chitosan is inexpensive, while the minimal content of silver ions in SCA1 (20.49 μg/mL) lowers the metal silver cost, making it suitable for scale-up production and application. Additionally, the Cage synthesis involves Schiff base reaction and reduction, which are easy to handle, and the starting materials are cheap. In the future, the detailed mechanisms of action, long-term safety, stability, and efficacy *in vivo* and *in vitro* will be studied to develop a novel antimicrobial agent using this immobilization strategy.

Credit authorship contribution statement

ZHOU Yiyu: Formal analysis, investigation, writing-original draft preparation; LIAN Zhifeng: Formal analysis, investigation, writing-original draft preparation; LÜ Yan, SUN Yiwei, and WU Huixiang: Software, validation; YANG Hua and HUANG Jianying: Conceptualization, writing-reviewing and editing.

References

[1] AHMAD A, WEI Y, SYED F, TAHIR K, REHMAN AU, KHAN A, ULLAH S, YUAN QP. The effects of bacteria-nanoparticles interface on the antibacterial activity of green synthesized silver nanoparticles[J]. Microbial Pathogenesis, 2017, 102: 133-142.

[2] 陈学情, 蒋家璇, 任志鸿, 李娟, 张红英, 徐建国, 杜华茂. 纳米银的抗菌特性及对多重耐药菌株的抗菌作用[J]. 微生物学报, 2017, 57(4): 539-549.
CHEN XQ, JIANG JX, REN ZH, LI J, ZHANG HY, XU JG, DU HM. Antibacterial activity of silver nanoparticles against multiple drug resistant strains[J]. Acta Microbiologica Sinica, 2017, 57(4): 539-549 (in Chinese).

[3] 李张强, 李娜, 李悦, 汪美贞. 贵金属纳米材料的抑菌机制[J]. 微生物学报, 2021, 61(2): 368-378.
LI ZQ, LI N, LI Y, WANG MZ. Antimicrobial noble metal-based nanomaterials[J]. Acta Microbiologica Sinica, 2021, 61(2): 368-378 (in Chinese).

[4] MEDICI S, PEANA M, CRISPONI G, NURCHI VM, LACHOWICZ JI, REMELLI M, ZORODDU MA. Silver coordination compounds: a new horizon in medicine[J]. Coordination Chemistry Reviews, 2016, 327: 349-359.

[5] WU HX, ZHANG YJ, CHEN H, LIU J, XIU LL, HUANG JY. Preparation, antioxidant and antibacterial activities of cryptate copper(II)/sulfonate chitosan complexes[J]. International Journal of Biological Macromolecules, 2023, 231: 123200.

[6] ZHAO FX, LIU YF, SONG T, ZHANG B, LI DX, XIAO YM, ZHANG XD. A chitosan-based multifunctional hydrogel containing *in situ* rapidly bioreduced silver nanoparticles for accelerating infected wound healing[J]. Journal of Materials Chemistry B, 2022, 10(13): 2135-2147.

[7] HUSAIN S, VERMA SK, HEMLATA, AZAM M, SARDAR M, HAQ QMR, FATMA T. Antibacterial efficacy of facile cyanobacterial silver nanoparticles inferred by antioxidant mechanism[J]. Materials Science and Engineering: C, 2021, 122: 111888.

[8] CHIEN YH, LIN BY, SHIH HH, CHEN CY, CHEN PC. The attract-kill inhibition mechanism in Ag/chitosan hydrogel for long-acting control of *Ralstonia solanacearum*[J]. Nanoscale, 2024, 16(45): 21077-21087.

[9] WANG P, WANG J, XIE ZL, ZHOU JX, LU QQ, ZHAO Y, DONG CJ, ZOU LL. Depletion of multidrug-resistant uropathogenic *Escherichia coli* BC1 by ebselen and silver ion[J]. Journal of Cellular and Molecular Medicine, 2020, 24(22): 13139-13150.

[10] ALICI EH, BILGIÇLI AT, GÜNSEL A, ARABACI G, NILÜFER YARASIR M. α-substituted phthalocyanines based on metal-induced H- or J-type aggregation for silver and palladium ions: synthesis, fluorescence, and antimicrobial and antioxidant properties[J]. Dalton Transactions, 2021, 50(9): 3224-3239.

[11] O'SHAUGHNESSY M, PIATEK M, McCARRON P, McCANN M, DEVEREUX M, KAVANAGH K, HOWE O. *In vivo* activity of metal complexes containing 1,10-phenanthroline and 3,6,9-trioxaundecanedioate ligands against *Pseudomonas aeruginosa* infection in *Galleria mellonella* larvae[J]. Biomedicines, 2022, 10(2): 222.

[12] LIU YH, JIANG Y, ZHU JL, HUANG JY, ZHANG HJ. Inhibition of bacterial adhesion and biofilm formation of sulfonated chitosan against *Pseudomonas aeruginosa*[J]. Carbohydrate Polymers, 2019, 206: 412-419.

[13] BHATIA N, KUMARI A, THAKUR N, SHARMA G, SINGH RR, SHARMA R. Phytochemically stabilized chitosan encapsulated Cu and Ag nanocomposites to remove cefuroxime axetil and pathogens from the environment[J]. International Journal of Biological Macromolecules, 2022, 212: 451-464.

[14] WANG B, WANG HM, WANG Z, TANG J, YUAN XT, ZHANG Y, CHEN HJ, YU WJ, SONG M. Preparation of AgBrNPs@copolymer-decorated chitosan with synergistic antibacterial activity[J]. Materials Today Communications, 2023, 37: 107482.

[15] FAN MN, SI JX, XU XG, CHEN LF, CHEN JP, YANG C, ZHU JW, WU LH, TIAN J, CHEN XY, MOU XZ, CAI XJ. A versatile chitosan nanogel capable of generating AgNPs *in situ* and long-acting slow-release of Ag^+ for highly efficient antibacterial[J]. Carbohydrate Polymers, 2021, 257: 117636.

[16] YANG H, JIN LQ, ZHAO DQ, LIAN ZF, APPU M, HUANG JY, ZHANG ZB. Antibacterial and antibiofilm formation activities of pyridinium-based cationic pillar [5] *Arene* against *Pseudomonas aeruginosa*[J]. Journal of Agricultural and Food Chemistry, 2021,

69(14): 4276-4283.
[17] SUN ZM, SHI CG, WANG XY, FANG Q, HUANG JY. Synthesis, characterization, and antimicrobial activities of sulfonated chitosan[J]. Carbohydrate Polymers, 2017, 155: 321-328.
[18] MÖLLER F, CASTAÑEDA-LOSADA L, JUNQUEIRA JRC, MILLER RG, REBACK ML, MALLICK B, van GASTEL M, APFEL UP. Modulation of the CO_2 fixation in dinickel azacryptands[J]. Dalton Transactions, 2017, 46(17): 5680-5688.
[19] ZHANG X, GENG XD, JIANG HJ, LI JR, HUANG JY. Synthesis and characteristics of chitin and chitosan with the (2-hydroxy-3-trimethylammonium) propyl functionality, and evaluation of their antioxidant activity *in vitro*[J]. Carbohydrate Polymers, 2012, 89(2): 486-491.
[20] BHATIA N, KUMARI A, CHAUHAN N, THAKUR N, SHARMA R. Duchsnea indica plant extract mediated synthesis of copper oxide nanomaterials for antimicrobial activity and free-radical scavenging assay[J]. Biocatalysis and Agricultural Biotechnology, 2023, 47: 102574.
[21] GIMENO P, BOUSQUET C, LASSU N, MAGGIO AF, CIVADE C, BRENIER C, LEMPEREUR L. High-performance liquid chromatography method for the determination of hydrogen peroxide present or released in teeth bleaching kits and hair cosmetic products[J]. Journal of Pharmaceutical and Biomedical Analysis, 2015, 107: 386-393.
[22] WANG L, PANG Y, SU ZW, XIN MH, LI MC, MAO YF. Synthesis of N-isonicotinic sulfonate chitosan and its antibiofilm activity against *E. coli* and *S. aureus*[J]. Carbohydrate Research, 2024, 542: 109194.
[23] SHIMADA K, FUJIKAWA K, YAHARA K, NAKAMURA T. Antioxidative properties of xanthan on the autoxidation of soybean oil in cyclodextrin emulsion[J]. Journal of Agricultural and Food Chemistry, 1992, 40(6): 945-948.
[24] 周士新, 陈越英, 徐燕. 爱洁杀菌消毒剂杀灭微生物效果及其影响因素[J]. 中国消毒学杂志, 2002, 19(3): 148-151.
ZHOU SX, CHEN YY, XU Y. Germicidal efficacy of ai-Jie germicidal disinfectant and its influencing factors[J]. Chinese Journal of Disinfection, 2002, 19(3): 148-151. (in Chinese).
[25] 何雨婧, 杜华茂. 靶向α-酮戊二酸脱氢酶增强纳米银的抗菌作用[J]. 微生物学报, 2024, 64(7): 2277-2294.
HE YJ, DU HM. Targeting alpha-ketoglutarate dehydrogenase enhances antibacterial activity of silver nanoparticles[J]. Acta Microbiologica Sinica, 2024, 64(7): 2277-2294 (in Chinese).
[26] 潘立博, 胡日新, 王靖宇, 王福金. 硝酸银与传统抗生素对常见细菌和真菌的杀菌能力比较[J]. 实验动物科学, 2014, 31(4): 41-45, 65.
PAN LB, HU RX, WANG JY, WANG FJ. Comparison of sterilization effect of silver nitrate with conventional antibiotics on bacteria and fungi[J]. Laboratory Animal Science, 2014, 31(4): 41-45, 65 (in Chinese).
[27] LOW WL, KENWARD K, BRITLAND ST, AMIN MC, MARTIN C. Essential oils and metal ions as alternative antimicrobial agents: a focus on tea tree oil and silver[J]. International Wound Journal, 2017, 14(2): 369-384.
[28] LOK CN, HO CM, CHEN R, HE QY, YU WY, SUN HZ, TAM PK, CHIU JF, CHE CM. Silver nanoparticles: partial oxidation and antibacterial activities[J]. JBIC Journal of Biological Inorganic Chemistry, 2007, 12(4): 527-534.
[29] RAY D, BHARADWAJ PK. Alteration in the binding property of a laterally nonsymmetric aza cryptand toward CuII, AgI, and TlI ions upon derivatization with a cyanomethyl group[J]. European Journal of Inorganic Chemistry, 2006, 2006(9): 1771-1776.
[30] MERMER A, ALYAR S. Synthesis, characterization, DFT calculation, antioxidant activity, ADMET and molecular docking of thiosemicarbazide derivatives and their Cu(II) complexes[J]. Chemico-Biological Interactions, 2022, 351: 109742.
[31] SIVASANKAR P, SEEDEVI P, POONGODI S, SIVAKUMAR M, MURUGAN T, SIVAKUMAR L, SIVAKUMAR K, BALASUBRAMANIAN T. Characterization, antimicrobial and antioxidant property of exopolysaccharide mediated silver nanoparticles synthesized by *Streptomyces violaceus* MM72[J]. Carbohydrate Polymers, 2018, 181: 752-759.
[32] KADAM D, MOMIN B, PALAMTHODI S, LELE SS. Physicochemical and functional properties of chitosan-based nano-composite films incorporated with biogenic silver nanoparticles[J]. Carbohydrate Polymers, 2019, 211: 124-132.
[33] SATHIYASEELAN A, SARAVANAKUMAR K, MARIADOSS AVA, WANG MH. Biocompatible fungal chitosan encapsulated phytogenic silver nanoparticles enhanced antidiabetic, antioxidant and antibacterial activity[J]. International Journal of Biological Macromolecules, 2020, 153: 63-71.